

General predictions for the neutron star crustal moment of inertia

Thomas Carreau,¹ Francesca Gulminelli,¹ and Jérôme Margueron²

¹*CNRS, ENSICAEN, UMR6534, LPC, F-14050 Caen cedex, France*

²*Institut de Physique Nucléaire de Lyon, CNRS/IN2P3, Université de Lyon, Université Claude Bernard Lyon 1, F-69622 Villeurbanne cedex, France*



(Received 18 October 2018; revised manuscript received 28 August 2019; published 11 November 2019)

The neutron star crustal equation of state and transition point properties are computed within a unified metamodeling approach. A Bayesian approach is employed including two types of filters: Bulk nuclear properties are controlled from low-density effective field-theory predictions as well as the present knowledge from nuclear experiments, whereas the surface energy is adjusted on experimental nuclear masses. Considering these constraints, a quantitative prediction of crustal properties can be reached with controlled confidence intervals and increased precision with respect to previous calculations: $\approx 11\%$ dispersion on the crustal width and $\approx 27\%$ dispersion on the fractional moment of inertia. The crust moment of inertia is also evaluated as a function of the neutron star mass, and predictions for mass and radii are given for different pulsars. The origin of Vela pulsar glitches is discussed, and a full crustal origin is excluded if we consider the present largest estimation of crustal entrainment. Further refinement of the present predictions requires a better estimation of the high-order isovector empirical parameters, e.g., K_{sym} and Q_{sym} , and a better control of the surface properties of extremely neutron rich nuclei.

DOI: [10.1103/PhysRevC.100.055803](https://doi.org/10.1103/PhysRevC.100.055803)

I. INTRODUCTION

The standard theory of pulsar glitches, this sudden spin-up of the rotational frequency of a compact star observed in almost 200 different pulsars since their discovery [1], assumes that the observed phenomenon originates from an abrupt transfer of angular momentum from the neutron superfluid to the solid crust of the star due to the unpinning of the superfluid vortices from the crystal lattice [2]. For this mechanism to justify the large glitches observed in some pulsars, such as Vela, the neutron star crust must be sufficiently thick to store a significant amount of angular momentum. The corresponding fraction of the crust moment of inertia I_{crust}/I can be estimated [3–5] in a range going from 1.6% up to 15%, depending on the importance of the effect of crustal entrainment, which is currently under debate [6,7].

A reliable estimation of the crust thickness and of the associated moment of inertia is, therefore, crucially needed to validate the crustal origin of pulsar glitches. This quantity is also a key parameter for the simulations of neutron star cooling [8]. For this estimation, constraints from low-energy nuclear physics appear more promising than direct constraints from astrophysics [9,10]. Indeed, the only poorly known parameter for the determination of the crustal thickness of a neutron star is the nuclear equation of state (EoS) and, most important, the density and pressure at the transition point from the solid crust to the liquid core [11].

In this paper, we present a unified EoS treatment [12–14] where the core and crust EoS are built within the same functional. To evaluate the uncertainties induced by the incomplete knowledge of the EoS, a metamodeling technique is used. It consists of generating a large set (10^8) of models

with fully independent model parameters using the strategy proposed in Refs. [15,16]. A similar metamodeling technique was already employed in Ref. [17]. In our paper, the priors are determined from nuclear phenomenology, and the probability distribution of the parameters is evaluated in a Bayesian approach by constraining energy and pressure in low-density (LD) homogeneous matter from a many-body perturbation theory (MBPT) based on two- and three-nucleon chiral effective field-theory (EFT) interactions at next-to-next-to-next-to-leading order and generating band predictions in isospin-symmetric and neutron matter [18].

Within the hypothesis of an analytic behavior of the pressure as a function of the density, the metamodel explores all types of density dependence for the EoS compatible with the imposed filters, in almost full independence with respect to any modeler constraints. The nuclear experimental and low-density theoretical uncertainties can, thus, be translated into quantitative predictions with controlled uncertainties for the crustal properties. If the effect of entrainment is additionally quantified, this can be further transformed into a prediction for the maximal glitch amplitude as a function of the neutron star mass.

The analytic behavior hypothesis of the present metamodeling technique implies that possible strong first-order phase transitions in the neutron star core are not accounted for. For this reason, we will mainly consider very light ($M = M_{\odot}$) and relatively light ($M = 1.4M_{\odot}$) neutron stars where such transitions are the least likely. We will show that the chiral EFT calculations impose very stringent constraints on the crust thickness and fractional moment of inertia. This is true, even if these calculations are limited to the low-density domain

$n \leq 0.2 \text{ fm}^{-3}$, and even for the canonical $M = 1.4M_{\odot}$ which is predicted to have a central density two to four times larger [16,19] than the nuclear saturation density $n_{\text{sat}} \approx 0.16 \text{ fm}^{-3}$.

A similar Bayesian study was very recently and independently performed in Refs. [20–22]. The same functional expression for the surface tension is used in the two approaches, but, at variance with Refs. [20–22], the surface tension parameters are, here, optimized for each EoS model on experimentally measured nuclear masses, and the uncertainty on the surface tension at extreme isospin values is, here, taken into account. Concerning the homogeneous part of the functional, our posterior distributions for the EoS is in very good agreement with the results of Ref. [22], showing the reliability and generality of the metamodeling technique.

II. FORMALISM

As discussed in the Introduction, the evaluation of the crust properties of a neutron star requires the knowledge of the crust-core transition density and pressure. They have been calculated by many authors using different versions of the density functional theory [11,23]. Most calculations are based on the thermodynamical spinodal, whereas this method provides only a qualitative estimation of the crust-core transition [24–26]. The limitation of the thermodynamical spinodal technique is easy to understand. Indeed, the transition occurs when the inhomogeneous phase becomes energetically favored over the homogeneous one [27]. This energy balance is governed by the interplay between the surface tension and the Coulomb energy. As a matter of fact, none of these terms contribute to the thermodynamical spinodal. A better estimation is obtained from the so-called dynamical spinodal [28], which corresponds to the instability border with respect to finite-size density fluctuations. Such calculations have, however, been performed for a small set of models [23–26]. Moreover, the crust-core transition in a steady nonaccreting neutron star is an equilibrium phenomenon, and it is not clear how precisely it can be addressed by an out-of-equilibrium spinodal calculation. For these reasons, in this paper, we will compute the transition point by directly comparing the free-energy density of uniform and clusterized matter.

Following Ref. [15], the generated metamodels are characterized by a set of empirical parameters $\{\vec{P}_{\alpha}\} = \{n_{\text{sat}}, K_{\text{sat}}, Q_{\text{sat}}, Z_{\text{sat}}, E_{\text{sym}}, L_{\text{sym}}, Q_{\text{sym}}, Z_{\text{sym}}, m^*, \Delta m^*, b\}$, corresponding to the successive density derivatives at saturation of the uniform matter binding energy in the isoscalar and isovector channels. They characterize the density dependence of the energy in symmetric matter and of the symmetry energy. An expansion up to the fourth order is necessary and sufficient to guarantee an excellent reproduction of existing functionals up to $4n_{\text{sat}}$, where n_{sat} is the saturation density of nuclear matter [15]. Two additional parameters rule the density dependence of the effective mass m^* and the effective-mass splitting Δm^* , and an extra b parameter enforces the correct behavior at zero density. This last parameter measures the low-density deviation from a Taylor expansion at saturation and turns out to be completely uninformative in this paper (see Fig. 4 below).

In the neutron star crust, the metamodeling is extended with a surface term, validated through comparisons with Thomas-Fermi calculations [29],

$$\sigma_s(x) = \sigma_0 \frac{2^{p+1} + b_s}{x^{-p} + b_s + (1-x)^{-p}}, \quad (1)$$

where x is the cluster proton fraction, see also Refs. [30,31]. The crust composition is then variationally determined within the compressible liquid drop model (CLDM) approximation [13,14,27,32].

The expression (1) for the surface tension requires three additional parameters. σ_0 and b_s are adjusted to reproduce experimental masses of spherical magic and semimagic nuclei: $^{40,48}\text{Ca}$, $^{48,58}\text{Ni}$, ^{88}Sr , ^{90}Zr , $^{114,132}\text{Sn}$, and ^{208}Pb .¹ The isovector surface parameter p determines the behavior of the surface energy for extreme isospin values, and it cannot be determined from experiments. In the following, we consider two different choices: either a fixed value $p = 3$ as suggested in Ref. [30] or including p in the parameter set $\{\vec{P}_{\alpha}\}$.

For each set of uniform matter parameters $\{\vec{P}_{\alpha}\}$, our fit provides optimal values for σ_0 and b_s , and the resulting χ^2 enters the Bayesian likelihood probability defined as

$$p_{\text{lik}}(\{\vec{P}_{\alpha}\}) = \mathcal{N} e^{-(1/2)\chi^2(\{\vec{P}_{\alpha}\})} \prod_{\alpha} g(\{\vec{P}_{\alpha}\}), \quad (2)$$

where the functions g are flat priors corresponding to a fully uncorrelated parameter set, which range is taken from Ref. [16], and \mathcal{N} is the normalization.

The posterior distribution is obtained by filtering the results of Eq. (2) imposing either physical constraints at high (supersaturation) density (HD) or *ab initio* EFT constraints at LD (subsaturation) or both (LD + HD),

$$p_{\text{post}}(\{\vec{P}_{\alpha}\}) = p_{\text{lik}}(\{\vec{P}_{\alpha}\}) \delta[\mathcal{F}(\{\vec{P}_{\alpha}\}) - \mathcal{F}_0], \quad (3)$$

where \mathcal{F}_0 is the chosen filter. The HD filter corresponds to the set of constraints: (i) positive symmetry energy up to M_{max} , (ii) stability of the EoS, (iii) causality up to the maximum mass, (iv) compatibility with the maximum observed masses $M_{\text{max}} \gtrsim 2M_{\odot}$ [33,34], see Ref. [16] for more details. We note that the possibility of a negative symmetry energy at high density was sometimes evoked in the literature [35,36]. We have checked that relaxing this condition does not modify any of the results presented in this paper. This can be explained by the fact that such ultrasoft functionals are generally incompatible with the $M_{\text{max}} \gtrsim 2M_{\odot}$ constraint. The LD filter retains only the EoS passing through the uncertainty band of the MBPT calculations of symmetric and neutron matter by Drischler *et al.* [18]. These calculations are considered in the density range of $0.05 \text{ fm}^{-3} < n < 0.2 \text{ fm}^{-3}$ where the perturbative chiral expansion is known to be fully reliable. Other *ab initio* calculations of pure neutron matter can be found in Refs. [37–39], which provide comparable theoretical band predictions. The use of a symmetric matter constraint is, however, important for the determination of the crust thickness because the transition is governed by isoscalar instabilities.

¹Enlarging the set of mass data does not modify the results.

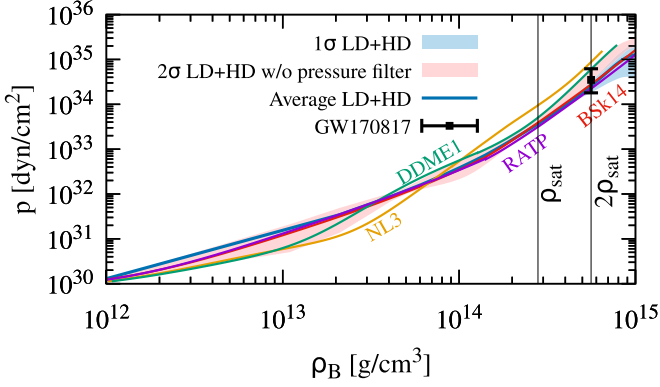


FIG. 1. Behavior of the equation of state retained by this paper compared to some popular models. The recent constraint from GW170817 [10] is also given.

Note that the HD filter implicitly implies that first-order phase transition does not occur in the star core up to $2M_{\odot}$ as the only hypothesis of the metamodeling is the analyticity of the EoS [15]. Therefore, imposing the LD filter alone might also be physically acceptable, and we will consider the two filters separately in the following.

III. RESULTS

The equation of state obtained in our paper is displayed in Fig. 1 and compared to some chosen models. In Fig. 1, the band noted “ 1σ LD + HD” represents the global filter, including both low-density and high-density constraints. For the LD constraint, we have imposed to the different functionals to respect the uncertainty bands of both the energy per particle and the pressure obtained in the chiral EFT calculation of symmetric matter and pure neutron matter. We can see that some popular models, notably the DD-ME1 and NL3 functionals issued from the relativistic mean-field theory, do not meet the final LD + HD prediction. If we relax the condition on the pressure of neutron matter, we obtain the band labeled “without pressure filter.” Even in this case, only a marginal agreement is obtained with the DD-ME1 and NL3 models at 2σ , showing that some tension exists between them and the *ab initio* calculation. Finally, the point in Fig. 1 gives the recent constraint from GW170817 [10]. We can see that this result is in very good agreement with our analysis.

The isovector surface parameter p plays an important role in the energetics of the inner crust [31] and may depart from its assumed value suggested in Ref. [30]. To determine a reasonable prior for p , we analyze its effect on the transition point. Figure 2 displays the transition density and pressure obtained for a set of relativistic and nonrelativistic functionals, in comparison with the dynamical spinodal calculation of Ref. [23]. We can see that values of the order $p \approx 3$ lead to a general good agreement with the instability analysis, and a variation ± 0.5 around $p = 3$ provides a good boundary for improved adjustment. In the case of the SLy4 functional, the value of $p = 2.61$ is needed to reproduce the unified EoS approach by Douchin and Haensel [32]; the lower value of

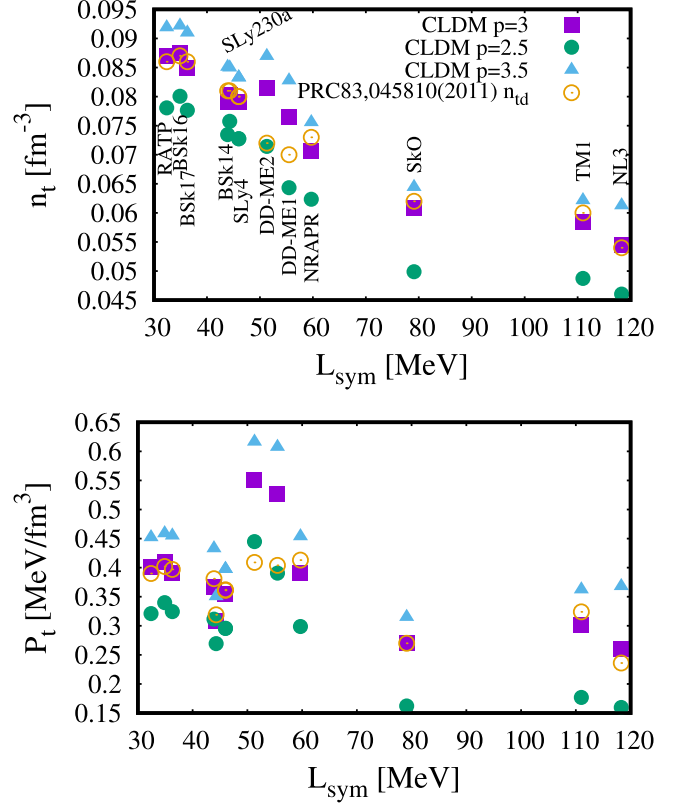


FIG. 2. Transition density n_t (top) and transition pressure P_t (bottom) as a function of L_{sym} for several interactions. The empty dots are the transition points calculated in Ref. [23] using the dynamical spinodal. The filled circles, squares, and triangles correspond to our estimation of the transition points with $p = 2.5$, $p = 3$, and $p = 3.5$, respectively.

p needed for DD-ME2 is in qualitative agreement with the TF calculations of Ref. [40].

Table I gives the average values and the standard deviations, defined as

$$\langle X \rangle = \sum_{\{\vec{P}_\alpha\}} X(\{\vec{P}_\alpha\}) p(\{\vec{P}_\alpha\}) \quad (4)$$

for a set of observables X for a canonical $1.4M_{\odot}$ neutron star. Fixing $p = 3$, we consider different probability distributions: the uncorrelated prior distribution $p(\{\vec{P}_\alpha\}) = \prod_{\alpha} g(\vec{P}_\alpha)$ (first line) or the posterior distribution Eq. (3) filtered according to the different constraints, $p(\{\vec{P}_\alpha\}) = p_{\text{post}}(\{\vec{P}_\alpha\})$, see rows 2 to 4. Knowing the transition point, a numerical solution of the Tolman-Oppenheimer-Volkoff equation allows computing the star radius, the thickness of the crust, and the crustal moment of inertia [11,41]. The first two moments of the distributions of these quantities are also reported in Table I. These results show that the high-density constraints are essential to establish the average crustal properties, but the knowledge of the low-density EoS is very constraining on the second moment of the distributions. Still, the transition pressure P_t and the fraction of crust moment of inertia have large uncertainties [42] on the order of 34% (respectively, 37%) considering the LD probability, decreasing to about 28% (respectively, 25%)

TABLE I. Average value and standard deviation of the transition density n_t , transition pressure P_t , central mass density ρ_c , radius R , crust thickness l_{crust} , and crustal fraction of moment of inertia for a $1.4M_\odot$ neutron star for different filters. We impose $p = 3$.

	n_t (fm^{-3})		P_t (MeV/fm^3)		$\rho_{c,1.4}(\times 10^{14})$ (g/cm^3)		$R_{1.4}$ (km)		$l_{\text{crust},1.4}$ (km)		$I_{\text{crust},1.4}/I_{1.4}$ (%)	
	Average	σ	Average	σ	Average	σ	Average	σ	Average	σ	Average	σ
Prior	0.089	0.037	0.310	0.340	6.661	1.102	12.77	0.61	1.13	0.29	3.40	3.34
HD	0.075	0.032	0.392	0.328	6.455	1.013	12.80	0.65	1.17	0.29	4.39	3.26
LD	0.074	0.011	0.364	0.122	7.820	1.075	11.94	0.42	0.95	0.11	3.54	1.33
LD + HD	0.077	0.010	0.389	0.111	6.756	0.606	12.47	0.25	1.03	0.10	4.50	1.25

if we additionally assume an analytical behavior of the EoS in the full density range covered by the observed neutron star (LD + HD, see fourth row in Table I).

As already stressed, the only hypothesis underlying the metamodelling is the analyticity of the EoS. This hypothesis might not be correct in the central part of the star if a strong first-order phase transition occurs. For this reason, we present in Table II the same quantities displayed in Table I, but this time for a very light $1.0M_\odot$ neutron star. We can see that the results on the transition point are fully compatible, whereas the crustal width and fractional moment of inertia decrease with decreasing mass as expected. Still, we cannot exclude that an extra source of uncertainty would arise for the higher masses if the possibility of nonanalyticities was accounted for. This work is currently under progress.

The correlation between the crustal width and its moment of inertia, which is the quantity connected to the maximal glitch amplitude, can be appreciated from the $1 - \sigma$ confidence ellipse [43] of Fig. 3 where the effect of the different constraints is also shown. Let us recall that the predictions labeled ‘‘Prior’’ here correspond to the consideration of nuclear experimental constraints, included as fully uncorrelated parameter sets. This figure shows that the LD prediction coming from *ab initio* nuclear theory is considerably less dispersed than the Prior or HD ones. The $2 - \sigma$ surface of the complete (LD + HD) prediction including all constraints correspond to a 84% confidence level.² Again, many popular

models give predictions which are not compatible with the present analysis when the LD constraints are accounted for.

This does not mean that the HD constraints are irrelevant in the determination of the neutron star properties: When the HD constraint is put on top of the LD one, see Table I, then it becomes clearer that the HD constraint has a non-negligible impact on other observables, such as the central density and 1.4-solar mass neutron star radius: It shifts the centroids produced by the LD constraint by a value which is about the second moment of the distribution, and it brings narrower widths. Surprisingly enough, this modification is also observed Table II, even if the HD constraint applies on the EoS behavior at densities higher than the central density of a 1-solar mass neutron star. Also, we can observe that the impact of varying the isovector surface parameter $p = \{2.5, 3, 3.5\}$ is quite large both in the $1 - \sigma$ confidence ellipse of Fig. 3 and in the star properties reported in Tables I and II.

Which empirical parameters contribute the most to the uncertainty in the observables shown in Fig. 3? To answer this question, the linear correlation coefficients $r_{XY} = \sigma_{XY}/(\sigma_X\sigma_Y)$ among the crustal thickness l_{crust} , the fractional moment of inertia I_{crust}/I , and the empirical parameters $\{\bar{P}_\alpha\}$ are shown in Fig. 4. Results for the different probability distributions previously considered are also shown. We can see that very similar values for r_{XY} are found for the two observables l_{crust} and I_{crust}/I . In general, we can observe that isovector empirical parameters are far more influential than the isoscalar ones as expected E_{sym} , K_{sym} , and Q_{sym} being the more influential parameters. The isoscalar parameters have also an effect on the curvature properties, e.g., K_{sat} , but their correlation coefficients are found to be weaker. It can

²This value deviates from the standard 90% because of non-Gaussianity of the probability distribution.

 TABLE II. The same as in Table I for a $1M_\odot$ neutron star.

	n_t (fm^{-3})		P_t (MeV/fm^3)		$\rho_{c,1.0}(\times 10^{14})$ (g/cm^3)		$R_{1.0}$ (km)		$l_{\text{crust},1.0}$ (km)		$I_{\text{crust},1.0}/I_{1.0}$ (%)	
	Average	σ	Average	σ	Average	σ	Average	σ	Average	σ	Average	σ
Prior	0.090	0.036	0.312	0.354	5.799	1.133	12.47	0.72	1.62	0.41	5.30	5.10
HD	0.075	0.032	0.393	0.329	5.625	0.962	12.52	0.72	1.69	0.42	6.96	4.91
LD	0.074	0.011	0.360	0.122	7.011	1.037	11.66	0.44	1.39	0.17	5.91	2.18
LD + HD	0.077	0.010	0.389	0.111	5.845	0.412	12.20	0.19	1.49	0.13	7.52	1.88

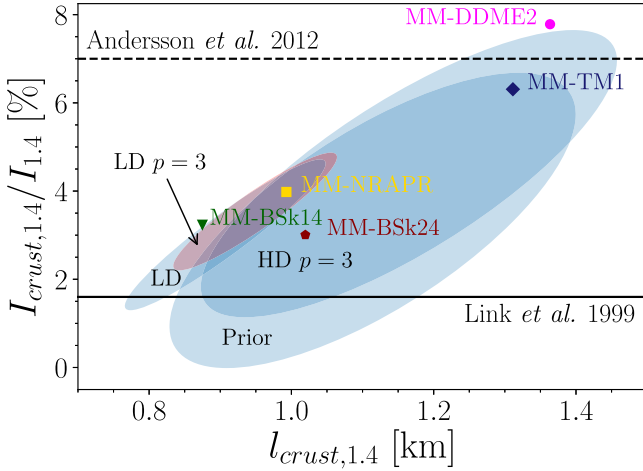


FIG. 3. A 1σ confidence ellipse for the crust thickness l_{crust} and the fraction of crust moment of inertia I_{crust}/I for a $1.4M_{\odot}$ neutron star with different filters (see the text). Minimal values needed to justify Vela glitches without (Link *et al.* 1999 [3]) and with (Andersson *et al.* 2012 [5]) entrainment are represented as well as the results from several popular models.

be explained by the fact that around saturation, the density derivative of the isoscalar binding energy—being related to the nuclear pressure—is small compared to the derivative of the symmetry energy. In more detail, the HD constraints do not impact the correlation coefficients, even if they are very selective: Only $\approx 1\%$ of the original parameter sets are retained. The absence of correlation with the L_{sym} parameter deserves some comments. It is well known that the NS radius R is well correlated to L_{sym} [12,41,42]. The same is true for the core radius R_{core} , explaining why the correlations cancel in the crustal thickness $l_{\text{crust}} = R - R_{\text{core}}$ and, consequently, on $I_{\text{crust},1.4}$. It then clearly appears that the higher-order parameters beyond L_{sym} must be better constrained to improve the prediction of the crustal properties.

Fixing p tends to increase those correlations as expected. However, if p is included in the parameter set, we can see that the uncertainty in the surface energy has an impact on the observables shown in Fig. 4 comparable to the one of the empirical parameters, see the LD row. This is a new feature which has not been reported by previous analyses.

Figure 4 also shows the correlation coefficients between observables. Large correlations are observed for the transition

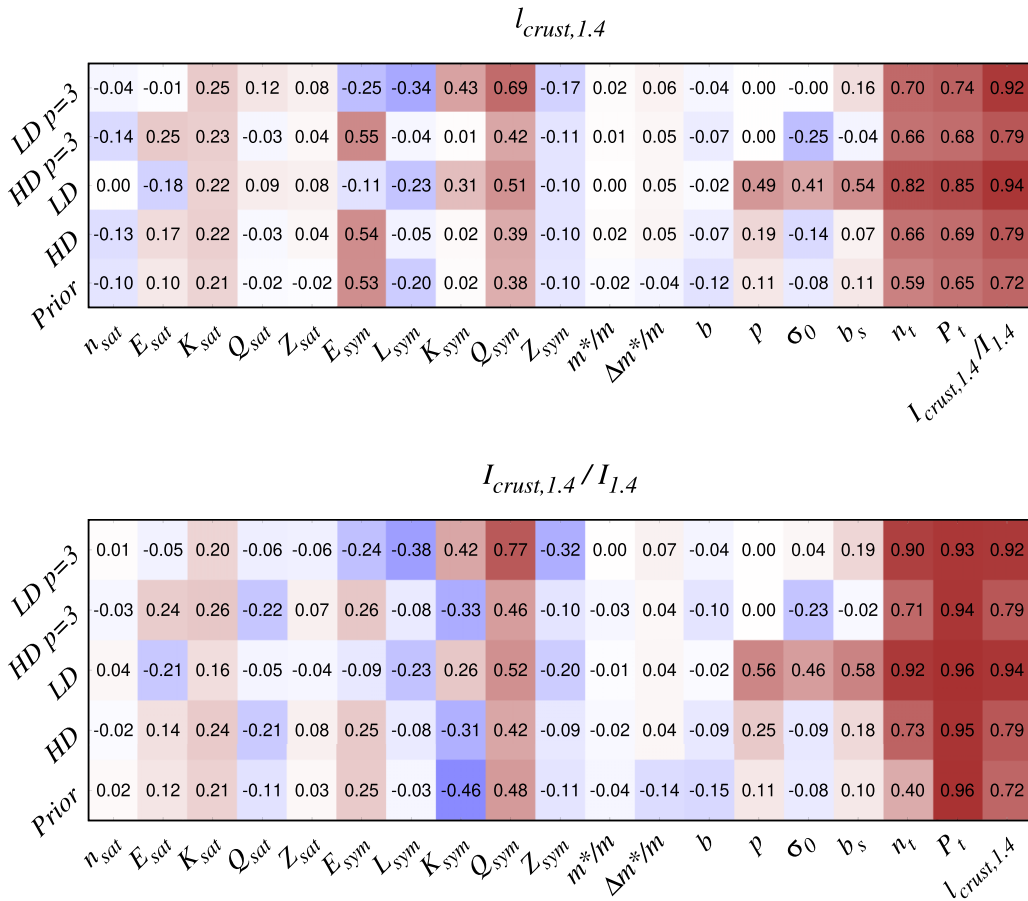


FIG. 4. Correlation between the crust thickness l_{crust} (top) and the fraction of crust moment of inertia I_{crust}/I (bottom) for a $1.4M_{\odot}$ neutron star with several parameters for different filters. The red (blue) color scale gives the intensity of the positive (negative) correlation, and the correlation coefficient is explicitly given for each parameter.

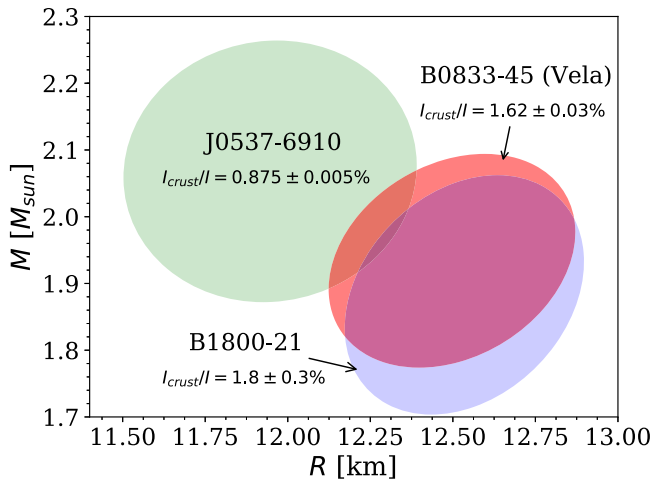


FIG. 5. A 1σ confidence ellipse with the LD + HD $p = 3$ filter for the mass and radius of different pulsars estimated from the observed glitch amplitude from Ref. [44] without crustal entrainment. The value of the crust fractional moment of inertia obtained from the whole statistical analysis (LD + HD constraints) is also given.

density and pressure as expected from previous studies, e.g., Ref. [11], and the correlation between $l_{\text{crust},1.4}$ and $I_{\text{crust},1.4}$ is also found to be very large, see Fig. 3.

Finally, Figs. 5 and 6 show the full impact of our present knowledge on the relation among the glitch amplitude, the fraction of crust moment of inertia I_{crust}/I , and the neutron star mass and radius.

Figure 5 displays one- σ confidence ellipses for three different pulsars estimated from the observed glitch amplitude from Ref. [44]. For this calculation, we have neglected possible entrainment effects and assumed that the observed glitches correspond to the maximum amplitude that can be sustained by the crust reservoir. This imposes the equality $G = I_{\text{crust}}/I$, where G is the measured glitch parameter [44]. The mass and

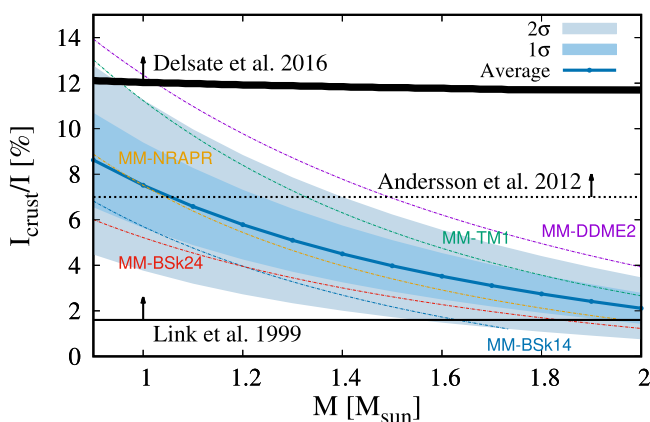


FIG. 6. Average fraction of crust moment of inertia I_{crust}/I as a function of the mass. The 1σ and 2σ confidence regions are represented as well as the minimum values needed to justify Vela glitches with (Delsate *et al.* [4] and Andersson *et al.* [5]) and without (Link *et al.* [3]) crustal entrainment.

radius distributions can then be computed as

$$p(M, R) = \sum_{\{\vec{P}_\alpha\}} p_{\text{post}}(\{\vec{P}_\alpha\}) \delta(M_\alpha - M) \delta(R_\alpha - R), \quad (5)$$

where M_α (R_α) represent the mass (radius) of a neutron star obtained with the parameter set $\{\vec{P}_\alpha\}$ when the central density is such that the corresponding fractional moment of inertia verifies $G = I_{\text{crust}}/I$. Here, G is sampled over a Gaussian distribution with average and variance taken from the measured values in Ref. [44].

The resulting confidence ellipses are larger than the ones obtained in Ref. [44]. This was expected since in that work a specific model for the EoS was supposed and the only uncertainty was the experimental one. However, the final results are roughly compatible with Ref. [44], showing that the experimental uncertainty on the glitch amplitude and the effect of the entrainment are dominant over the EoS uncertainty.

Note that an innovative method was proposed to determine the mass and radius using observations of the maximum observed glitches [45]. It would be interesting to compare this approach with ours.

Finally Fig. 6 gives a complete study of the effect of entrainment in the case of Vela: The average value of the fraction of crust moment of inertia I_{crust}/I is shown as well as the boundaries of the 1σ and 2σ probabilities. The different black lines represent the values proposed with [4,5] and without [3] the entrainment effect on the crust moment of inertia to explain Vela glitches. From Fig. 6, we can conclude that the value determined for the maximal entrainment effect is incompatible with the present nuclear physics knowledge if we keep the standard picture where superfluidity is limited to the crust.

IV. CONCLUSIONS

In conclusion, considering the experimental and EFT theoretical predictions at low density, the uncertainty on the crust thickness (relative moment of inertia) is on the order of 9% (25%) for $M = 1.4M_\odot$. These uncertainties originate from the dispersion in the predictions of the crust-core transition point, which, in turn, depends on the high-order isovector empirical parameters K_{sym} and Q_{sym} , as well as on the isovector surface energy parameter p . Higher precision in the experimental determination of K_{sym} and Q_{sym} in the low-density EFT theoretical predictions and in the microscopic modeling of the surface energy at extreme isospin ratios are needed to reduce the uncertainties of crustal observables. Concerning this last point, extended Thomas-Fermi calculations with the metamodeling technique are in progress in order to fix the functional dependence of the p parameter.

ACKNOWLEDGMENTS

This work was partially supported by the IN2P3 Master Project MAC “NewCompStar” COST Action Project No. MP1304 and PHAROS COST Action Project No. MP16214.

- [1] C. M. Espinoza, A. G. Lyne, B. W. Stappers, and M. Kramer, *Mon. Not. R. Astron. Soc.* **414**, 1679 (2011).
- [2] B. Haskell and A. Melatos, *Int. J. Mod. Phys. D* **24**, 1530008 (2015).
- [3] B. Link, R. I. Epstein, and J. M. Lattimer, *Phys. Rev. Lett.* **83**, 3362 (1999).
- [4] T. Delsate, N. Chamel, N. Gurlebeck, A. F. Fantina, J. M. Pearson, and C. Ducoin, *Phys. Rev. D* **94**, 023008 (2016).
- [5] N. Andersson, K. Glampedakis, W. C. G. Ho, and C. M. Espinoza, *Phys. Rev. Lett.* **109**, 241103 (2012).
- [6] N. Martin and M. Urban, *Phys. Rev. C* **94**, 065801 (2016).
- [7] G. Watanabe and C. J. Pethick, *Phys. Rev. Lett.* **119**, 062701 (2017).
- [8] D. Page and S. Reddy, *Phys. Rev. Lett.* **111**, 241102 (2013).
- [9] W. G. Newton, J. Hooker, M. Gearheart, K. Murphy, D.-H. Wen, F. J. Fattoyev, and B.-A. Li, *Eur. Phys. J. A* **50**, 41 (2014).
- [10] B. P. Abbot *et al.*, *Phys. Rev. Lett.* **121**, 161101 (2018).
- [11] J. Piekarewicz, F. J. Fattoyev, and C. J. Horowitz, *Phys. Rev. C* **90**, 015803 (2014).
- [12] M. Fortin, C. Providência, A. R. Raduta, F. Gulminelli, J. L. Zdunik, P. Haensel, and M. Bejger, *Phys. Rev. C* **94**, 035804 (2016).
- [13] B. K. Sharma, M. Centelles, X. Viñas, M. Baldo and G. F. Burgio, *Astron. Astrophys.* **584**, A103 (2015).
- [14] H. Shen, H. Toki, K. Oyamatsu, and K. Sumiyoshi, *Nucl. Phys. A* **637**, 435 (1998).
- [15] J. Margueron, R. Hoffmann Casali, and F. Gulminelli, *Phys. Rev. C* **97**, 025805 (2018).
- [16] J. Margueron, R. Hoffmann Casali, and F. Gulminelli, *Phys. Rev. C* **97**, 025806 (2018).
- [17] A. W. Steiner, J. M. Lattimer, and E. F. Brown, *Astrophys. J. Lett.* **765**, 5 (2013).
- [18] C. Drischler, K. Hebeler, and A. Schwenk, *Phys. Rev. C* **93**, 054314 (2016).
- [19] S. Gandolfi, J. Carlson, S. Reddy, A. W. Steiner, and R. B. Wiringa, *Eur. Phys. J. A* **50**, 10 (2014).
- [20] Y. Lim and J. W. Holt, *Phys. Rev. Lett.* **121**, 062701 (2018).
- [21] Y. Lim, J. W. Holt, and R. J. Stahulak, *Phys. Rev. C* **100**, 035802 (2019).
- [22] Y. Lim and J. W. Holt, [arXiv:1902.05502](https://arxiv.org/abs/1902.05502).
- [23] For a compilation of different relativistic and non-relativistic approaches, see C. Ducoin, J. Margueron, C. Providencia, and I. Vidana, *Phys. Rev. C* **83**, 045810 (2011).
- [24] H. Pais, A. Sulaksono, B. K. Agrawal, and C. Providencia, *Phys. Rev. C* **93**, 045802 (2016).
- [25] C. Ducoin, P. Chomaz, and F. Gulminelli, *Nucl. Phys. A* **789**, 403 (2007).
- [26] J. Xu, L.-W. Chen, B.-A. Li, and H.-R. Ma, *Astrophys. J.* **697**, 1549 (2009).
- [27] G. A. Baym, H. A. Bethe, and C. J. Pethick, *Nucl. Phys. A* **15**, 225 (1971).
- [28] C. J. Pethick, D. G. Ravenhall, and C. P. Lorentz, *Nucl. Phys. A* **584**, 675 (1995).
- [29] D. G. Ravenhall, C. J. Pethick, and J. M. Lattimer, *Nucl. Phys. A* **407**, 571 (1983).
- [30] C. P. Lorenz, D. G. Ravenhall, and C. J. Pethick, *Phys. Rev. Lett.* **70**, 379 (1993).
- [31] W. G. Newton, M. Gearheart, and B.-A. Li, *Astrophys. J. Suppl. Ser.* **204**, 9 (2013).
- [32] F. Douchin and P. Haensel, *Astron. Astrophys.* **380**, 151 (2001).
- [33] J. Antoniadis, P. Freire, N. Wex *et al.*, *Science* **340**, 1233232 (2013).
- [34] Z. Arzoumanian, A. Brazier, S. Burke-Spolaor *et al.*, *Astrophys. J., Suppl. Ser.* **235**, 37 (2018).
- [35] B. A. Li, in *Exotic Nuclei and Nuclear/Particle Astrophysics (VI). Physics with Small Accelerators: Proceedings of Carpathian Summer School of Physics 2016 (CSSP16)*, edited by L. Trache and D. G. Ghita, AIP Conf. Proc. No. 1852 (AIP, New York, 2017).
- [36] R. B. Wiringa, V. Fiks, and A. Fabrocini, *Phys. Rev. C* **38**, 1010 (1988).
- [37] I. Tews, S. Gandolfi, A. Gezerlis, and A. Schwenk, *Phys. Rev. C* **93**, 024305 (2016).
- [38] J. W. Holt and N. Kaiser, *Phys. Rev. C* **95**, 034326 (2017).
- [39] I. Tews, J. Carlson, S. Gandolfi, and S. Reddy, *Astrophys. J.* **860**, 149 (2018).
- [40] F. Grill, C. Providencia, and S. S. Avancini, *Phys. Rev. C* **85**, 055808 (2012).
- [41] J. M. Lattimer and M. Prakash, *Phys. Rep.* **333**, 121 (2000).
- [42] A. W. Steiner, S. Gandolfi, F. J. Fattoyev, and W. G. Newton, *Phys. Rev. C* **91**, 015804 (2015).
- [43] M. Friendly, G. Monette, and J. Fox, *Stat. Sci.* **28**, 1 (2013).
- [44] W. C. G. Ho, C. M. Espinoza, D. Antonopoulou, and N. Andersson, *Sci. Adv.* **1**, e1500578 (2015).
- [45] P. M. Pizzochero, M. Antonelli, B. Haskell, and S. Seveso, *Nat. Astron.* **1**, 0134 (2017).